

# Evaluating the Change in Fingerprint Directional Patterns under Variation of Rotation and Number of Regions

Kribashnee Dorasamy<sup>1,2</sup>, Leandra Webb<sup>1</sup> and Jules Tapamo<sup>2</sup>

<sup>1</sup>CSIR, Modelling and Digital Science,

P.O. Box 395, Building 17B, Pretoria, 0001, South Africa

<sup>2</sup>School of Engineering, Howard College, University of KwaZulu-Natal,

King George V Avenue, Durban, 4041, South Africa

KDorasamy@csir.co.za, LWebb@csir.co.za, tapamoj@ukzn.ac.za

**Abstract:** Directional patterns (DPs), which are formed by grouping regions of orientation fields falling within a specific range, vary under rotation and the number of regions. For fingerprint classification schemes, this can result in misclassification due to inconsistency of patterns. Knowing the optimal angle by which to rotate the image and the optimal number of orientation regions to divide it into can be beneficial in analysing specific properties of a class. Furthermore, the number of regions directly impacts singular point (SP) detection, therefore using the optimal number of regions prevents loss of SPs. However, no previous work justifies the use of a specific number of regions or angle of rotation. More so, no explicit studies have been conducted to establish the optimal number of regions or angle of rotation that result in gaining the most information from a pattern. Therefore, this research investigates the change in DPs under the variation of rotation and number of regions to determine which condition provides the best representation of the fingerprint that is less prone to noise and minimizes interclass variability issues with fewer possible patterns for each class. This can serve as a baseline for future works using DPs. The experiments were conducted on the Fingerprint Verification Competition (FVC) 2002 database (DB) 1a. It was found that using a small number of regions produces the most accurate SPs detection and increasing the region number to more than 6 regions drastically depletes the accuracy of SP detection. Furthermore, aligning the SPs of a fingerprint containing a single loop and delta, highlights the essential properties of a class better, with fewer layouts for each class.

## 1 Introduction

Exclusive classification is one of the processes applied in fingerprint recognition systems to decrease the ratio of penetration, in which comparisons are only made against fingerprints which have a common pattern. Galton defined these patterns as classes, namely Whorl (W), Right Loop (RL), Left Loop (LL), Tented Arch (TA) and Plain Arch (PA) [Gal91]. Recently, directional pattern (DP) techniques, stemming from the popular structural approach, have been commonly used in fingerprint classification [LHH08, DWTK15]. In this technique, the arrangement of regions composed of a specific range of orientation fields forms a pattern, known as a DP. Each fingerprint class is represented by a unique DP, which can be used for classification. Globally analysing the arrangement of the regions that constitute a DP of a specific class provides more information about the structural properties of that class, than the traditional structural features. These attributes have

proven to be advantageous in solving common challenges, inclusive of noise, by moving away from the uncertainty of local orientation fields [DWTK15]. In addition, this technique has the potential to classify fingerprints that are not fully captured resulting in loss of singular points (SPs), a very critical issue that is caused from incorrect finger placement on scanners [DWTK15].

To achieve the maximum potential of this technique, DPs have to be consistent for each class. This can be achieved by using the optimal number of regions at a rotation that best emphasises the characteristics of a class. However, classification techniques that have used this fingerprint feature have not undertaken any explicit study examining the ideal conditions of DPs and researchers have not provided reasoning behind the choice of a specific number of regions and rotation [WBS12, LHH08, BKAM13].

Generally many practitioners use three [LHH08, DWTK15] and four [WBS12, MM96, CMM02] region partitions for DPs. Wang *et al.* stated that 4 regions were used as it provides sufficient information to locate SPs and sizes of the regions make it easier to validate a true SP [WBS12]. The authors also claim that eliminating excess noise becomes difficult as the number of regions increases to more than eight partitions [WBS12]. However, no experiments were conducted to justify his statement.

Liu *et al.* and Dorasamy *et al.* both use a DP technique for classification, however the way in which the fingerprints are rotated differ [LHH08, DWTK15]. For each method, unique DPs were produced, showing that they vary under rotation. This inconsistency of patterns can lead to excess amounts of computation. Finding an optimal rotation that has less layouts for each class and distinct patterns that are less prone to noise and interclass variability issues could reduce misclassification and computational cost.

In this paper, the impact of varying the number of regions and rotation of a DP is analysed to establish the optimal number of regions and rotation for classification. The ideal way to test this would be to implement a number of classification schemes for each number of regions and rotation. However, most automated schemes are specific to a single number of regions, and class patterns vary for different numbers of regions and segmentation strategies. Therefore visual comparisons are made of changes in patterns instead.

The following sections present the details of the experiments and the analysis on the impact of the variation of number of regions and rotation of DPs. The description of the methodology is discussed in Section 2. Section 3 provides the discussion of the findings obtained from the change in DPs, influenced by fingerprint rotation and varying the number of regions. Based on the findings, Section 4 states the recommendations on the number of regions and amount of rotation that can be used as a baseline. The conclusions are summarised in Section 5.

## 2 Experimental Set-up

In order to assess the impact of varying the number of regions and varying rotation, two stages of experiments were carried out. The first assessed the impact of varying the number of regions and the second varying the rotation. The details of the two stages are covered in Section 2.1 and 2.2, respectively.

## 2.1 Experimental set-up for the variation of number of regions

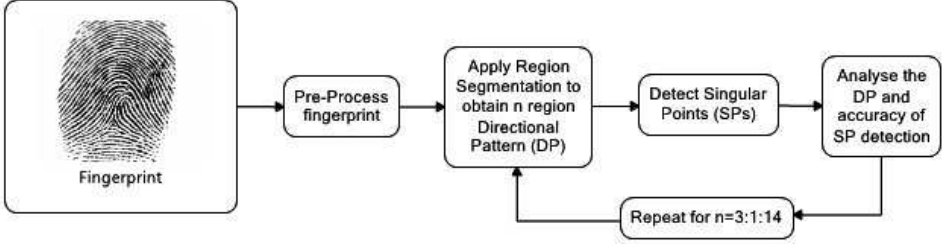


Figure 1: Overview of the experimental set-up for varying the number of regions

Figure 1 shows the overview of the process undertaken to conduct the analysis of the variation of the number of regions. An input fingerprint is initially pre-processed to eliminate the background in the fingerprint image. The orientation fields were computed in the region segmentation stage, where they were grouped into  $n$  homogeneous regions to form a DP. The uniqueness of the pattern and accuracy of the SPs were then observed. The region segmentation, SP detection and observation were repeated with  $n$  being varied from 3 to 14. The pre-processing, region segmentation, SP detection and the observation are further discussed in Section 2.1.1, Section 2.1.2, Section 2.1.3, and Section 2.1.4, respectively.

### 2.1.1 Pre-Processing

In this step, the foreground which includes the ridges and valleys of a fingerprint are separated from the background. The segmentation is performed using the method in [WBG10].

### 2.1.2 Region segmentation

The orientation fields within a specific range  $range_i$  are grouped and assigned a particular region number to form a DP, as shown in Figure 2. The orientation map is represented by a matrix  $Orient(r, c)$ , where  $r$  is the row and  $c$  is the column of the fingerprint image. The computation of the orientation map is covered in [HWJ98], in which the axis advances clockwise from  $0^\circ$  to  $180^\circ$ . To reduce local orientation uncertainty, smoothing is applied using a Gaussian filter. The interval and ranges of each region used to form a DP, are computed using the formulae in Equations 1 to 3 [DWT15]. Equation 1 is used to obtain the step  $\Delta\phi$  in which the region is discretized into, where  $n$  is the number of regions.

$$\Delta\phi = \pi/n \quad (1)$$

Regions are formed by grouping the orientation fields within a specific range. This range is computed using Equation 2, where  $i = 1 \dots n$ .

$$range_i = [(i-1) * \Delta\phi] : [i * \Delta\phi] \quad (2)$$



Figure 2: The DP of a particular fingerprint, using three orientation ranges [DWTK15]

Figure 2 depicts region numbers on a DP, at a specific location  $(r, c)$  that is obtained using Equation 3, where  $Orient$  is the orientation value at location  $(r, c)$ .

$$region_{num}(r, c) = \lceil Orient(r, c) / \Delta \phi \rceil \quad (3)$$

### 2.1.3 Singular point detection

The point of intersection between  $n$  regions on a DP, indicates SPs [DWTK15]. The intersection may not always occur at a single point, so a neighbour of 24 or 48 pixels is searched instead, referred to here as 24 ND and 48 ND. Figure 3 (a) shows an example used to indicate an SP by detecting 3 different pixel values, within a 5x5 matrix (24 ND) and around location  $region_{num}(r, c)$ . Loops are identified by regions advancing in a counter-clockwise direction and deltas are represented by regions flowing in a clockwise direction, as illustrated in Figure 3. The coordinates of the loop and delta were compared to a ground truth of manually located SPs.

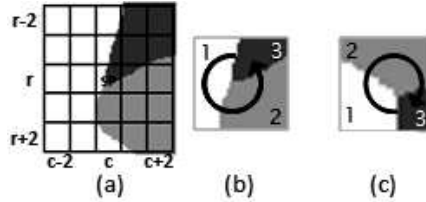


Figure 3: Points of a three region intersection representing (a) SP using a 24 ND, (b) loop and (c) delta [DWTK15]

### 2.1.4 Observation made on the DP

To assess the effect of varying the number of regions, the accuracy of the SP detection is observed as the number of regions are varied. In addition, the pattern of a noisy fingerprint is analysed, as the number of regions are increased.

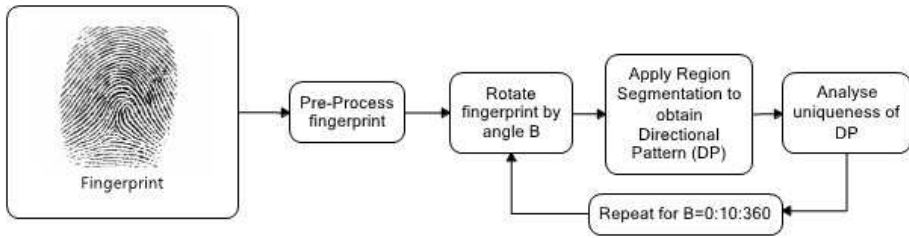


Figure 4: Overview of the experimental set-up for varying angle of rotation

## 2.2 Experimental set-up for the variation of rotation

Figure 4 shows the overview of the process carried out to perform the study on variation of DPs under rotation. Fingerprints are pre-processed to remove the excess background of the image and the fingerprint is rotated by a specified amount. Once the image is rotated, the region segmentation is applied. The change in DP is then observed. The pre-processing and region segmentation algorithm was covered in Section 2.1.1 and Section 2.1.2, respectively. Section 2.2.1 provides the details of obtaining the amount which the image is rotated by. The method of observation is concluded in Section 2.2.2.

### 2.2.1 Increments for rotation

Fingerprints are rotated by an angle  $B$ , where  $B$  increments every  $10^\circ$ , from  $0^\circ$  to  $360^\circ$ . The increment of  $10^\circ$  was selected since it is a small rotational value allowing the observation of the subtle change of a DP.

### 2.2.2 Observation made on the DP

Rotation changes the layout of a DP. To assess the effect of varying rotation, the uniqueness of the pattern is manually observed as the fingerprint is rotated.

## 2.3 Testing Samples

To conduct the experiment 1 as illustrated in Figure 1, fingerprint images from the Fingerprint Verification Competition (FVC) 2002 database (DB)1a were selected [MMC<sup>+</sup>02]. Of the 100 finger impressions contained in FVC 2002 DB1a, 63 upright complete fingerprints were chosen, due to the manual analysis required for experiment 2 depicted in Figure 4.

## 3 Discussion

### 3.1 Variation of the number of regions

The effects of varying the number of regions is observed in terms of SP accuracy and pattern consistency.

### 3.1.1 Impact of the variation of the number of regions on SP accuracy

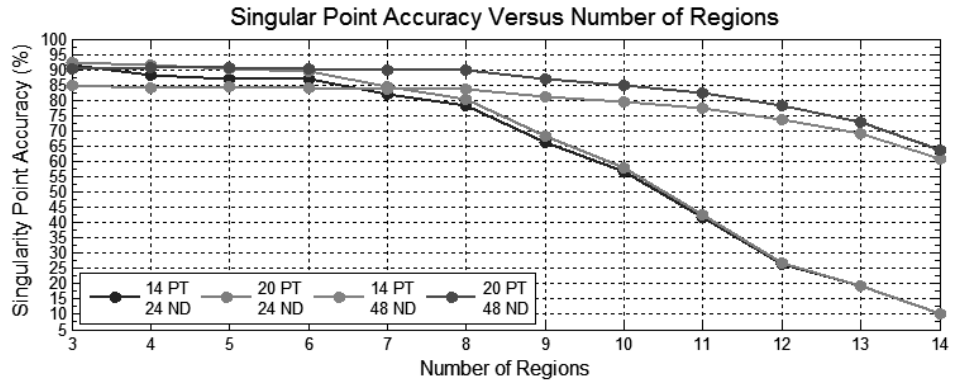


Figure 5: Accuracy of singular points (SPs) versus number of regions

Figure 5 shows the accuracy of SPs detected on a fingerprint for a specific number of regions. The SP detection accuracy is seen to decrease as the number of regions increases from 3 to 14. Four different tests were conducted by varying the pixel tolerance (PT) and ND values. The PT value is the maximum number of pixels that the automatically detected SP can be from the true SP location to still be considered correct. Two different PT values were tested. A PT of 14 is applied to accommodate human error when obtaining the ground truth values. A larger PT of 20 was also selected to evaluate the impact of pixel distortion, resulting in a larger deviation from the location of the ground truth results. Two NDs were observed, a 24 ND since it was the smallest ND that can detect SPs of the largest number of regions under observation; and a 48 ND was used to analysis the impact of pixel distortion on the final accuracy. If any false SPs occurred or any true SPs were not detected, it is considered to be an incorrect detection. From the graph, it is observed that when the number of regions is greater than 6, all lines experience a drop in accuracy, therefore a smaller number of regions is better.

An example of a W fingerprint directional pattern with 15 regions is shown in Figure 6, zoomed in to illustrate the reason for the rapid decrease in SP detection for higher number of regions. From observation all regions don't converge at a single point. Increasing the ND from 24 to 48 can elevate this problem which can be shown by the higher accuracy for 6 to 14 regions. However, using the larger ND range can result in SPs being further from the true SP, therefore a higher PT of 20 shows an increase in the overall accuracy. This indicates that the located SP is 20 pixels off from the true SP. When observing Figure 6 (b), if the ND is too small, all regions may not be detected for larger number of regions, hence the sudden drop from 6 to 14 regions when using a 24 ND. However, even with a high ND and PT, a small number of regions consistently produces better accuracy for all four cases, since there is less distortion and therefore the detected location is generally closer to the true location. A 3 region DP with 14 PT using 24 ND, having a high overall accuracy of 91.38% with a minimum PT, was the optimal output.

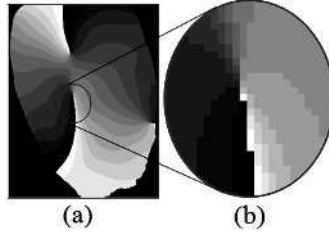


Figure 6: Illustration for the reason for decreased SP detection with a high region number, (a) shows a W with 15 regions and (b) shows the intersection of a 15 region W, which is not a single point

### 3.1.2 Impact of the variation of the number of regions on noisy images

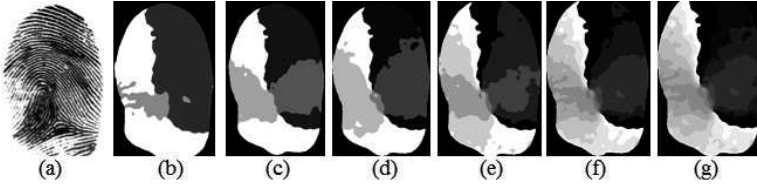


Figure 7: Noisy fingerprint image with different number of regions, (b) 3, (c) 4, (d) 5, (e) 7, (f) 12 and (g) 15

For this case, the smoothing of orientation fields was removed in the pre-processing stage in order to observe how the number of regions affects noise in the DP. Figure 7 (a) depicts a LL containing smudges and missing ridges. The number of regions was varied to observe the behaviour of noise. When the amount of regions increased, the amount of noise increased. For three region segmentation, the least amount of noise is detected and the pattern is more distinct. Therefore, a smaller number of regions is advantageous to both SP detection and noise reduction, as it is likely to encounter false SPs or loss of SPs.

## 3.2 Variation of the amount of rotation

To observe the effect of varying rotation, the pattern changes of each class were observed as the images were rotated. Only the angles at which the fingerprint DP changes the most will be depicted in the figures used in this section.

### 3.2.1 Observation of the PA DP under rotation

Figure 8 (b) - Figure 8 (g) shows the DPs of a PA as the angle is varied. The PA fingerprint has unique structural properties containing no SPs, resulting in the regions never intersecting at any rotation. Therefore, for the PA class, there is no optimal rotation as the pattern can easily be identified for any rotation.



Figure 8: The different patterns of a PA under rotation where the fingerprint is rotated at angles of, (b)  $0^\circ$ , (c)  $20^\circ$ , (d)  $30^\circ$ , (e)  $40^\circ$ , (f)  $60^\circ$  and (g)  $90^\circ$

### 3.2.2 Observation of the W DP under rotation

Figure 9 shows a W fingerprint rotated at angles, (b)  $0^\circ$ , (c)  $10^\circ$ , (d)  $30^\circ$ , (e)  $50^\circ$  and (f)  $90^\circ$ . The DP of a W produces the most consistent pattern compared to RL, LL and TA, due to its symmetrical structure between the top and bottom loop. This forms a single common region between all SPs. Only the region number of the common region changes under rotation. Hence, any rotation is suitable. However, it was found that region loss occurs at the bottom loop, when the fingerprint was at an angle other than  $0^\circ$ ,  $90^\circ$ ,  $180^\circ$ ,  $270^\circ$  and  $360^\circ$ . Therefore, the most reliable patterns are produced at approximate angles of  $0^\circ$ ,  $90^\circ$ ,  $180^\circ$ ,  $270^\circ$  and  $360^\circ$ .

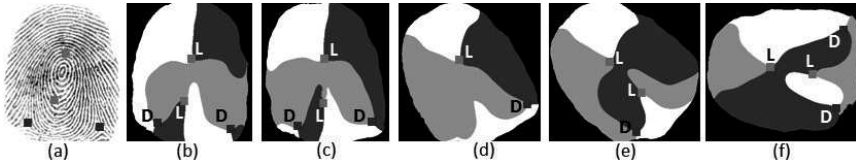


Figure 9: The DPs of a W under rotation, where the fingerprint is rotated at angles of, (b)  $0^\circ$ , (c)  $10^\circ$ , (d)  $30^\circ$ , (e)  $50^\circ$  and (f)  $90^\circ$

### 3.2.3 Observation of the RL, LL and TA DPs under rotation

Since RLs, LLs and TAs have one loop and one delta, these fingerprints were analysed simultaneously. Analysing all the RL, LL and TA DPs produced for angles  $0^\circ$  to  $360^\circ$ , revealed that different layouts were formed for different angles. These layouts differ in the number of regions that link the loop and delta which will be referred to as Common Regions (CRs).

Both RLs and LLs produce three different layouts based on the number of CRs, as shown in Figure 10 and 11. The three layouts of a RL and LL are 3 CR, 2 CR and 1 CR. For a TA only two layouts, 3 CRs and 2 CRs can be produced, as seen in Figure 12. In this section, the changes of the DP of each type of layout of the various classes are analysed to determine the optimal rotation. Since a small rotational change of approximately  $5^\circ$  can result in a DP of a 3 CR TA converting to a 2 CR TA, it was only necessary to analyse one of these two layouts. The 3 CRs TA was used for analysis.

Unlike W and PA fingerprints, patterns for a RL, LL and TL are not consistent. Figures





Figure 10: Three DP layouts of a RL namely, (a) RL which produces a 3 CR layout, (b) 3 CR layout, (c) RL which produces a 2 CR layout, (d) 2 CR layout, (e) RL which produces a 1 CR layout and (f) 1 CR layout

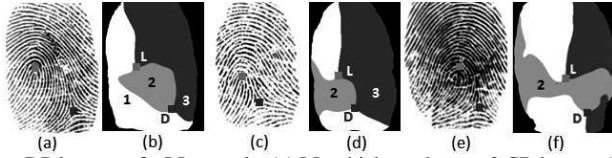


Figure 11: Three DP layouts of a LL namely, (a) LL which produces a 3 CR layout, (b) 3 CR layout, (c) LL which produces a 2 CR layout, (d) 2 CR layout, (e) LL which produces a 1 CR layout and (f) 1 CR layout

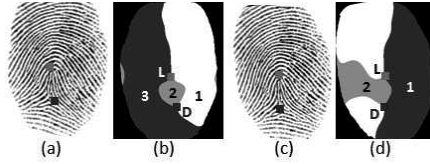


Figure 12: Two DP layouts of a TA namely, (a) TA which produces a 3 CR layout, (b) 3 CR layout, (c) TA which produces a 2 CR layout and (d) 2 CR layout

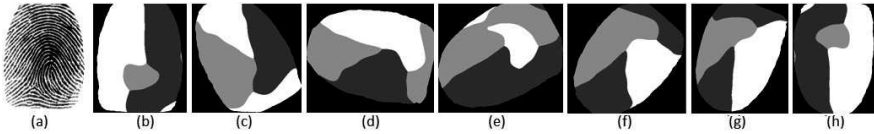


Figure 13: The different patterns produced when a 3 CR RL undergoes rotation at angles of (b)  $0^\circ$ , (c)  $30^\circ$ , (d)  $80^\circ$ , (e)  $120^\circ$ , (f)  $140^\circ$ , (g)  $160^\circ$  and (h)  $180^\circ$

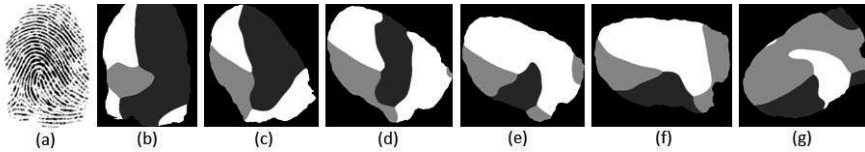


Figure 14: The DPs produced when a 2 CR RL undergoes rotation at angles of (b)  $0^\circ$ , (c)  $20^\circ$ , (d)  $50^\circ$ , (e)  $60^\circ$ , (f)  $80^\circ$  and (g)  $120^\circ$

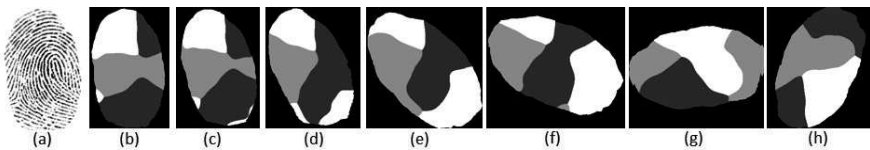


Figure 15: The different patterns produced when a 1 CR RL undergoes rotation at angles of (b)  $0^\circ$ , (c)  $10^\circ$ , (d)  $20^\circ$ , (e)  $30^\circ$ , (f)  $60^\circ$ , (g)  $90^\circ$  and (h)  $150^\circ$

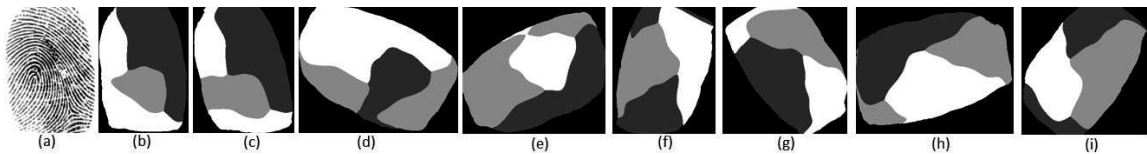


Figure 16: The different patterns produced when a 3 CR LL undergoes rotation at angles of (b)  $0^\circ$ , (c)  $10^\circ$ , (d)  $60^\circ$ , (e)  $110^\circ$ , (f)  $160^\circ$ , (g)  $210^\circ$ , (h)  $280^\circ$  and (i)  $320^\circ$

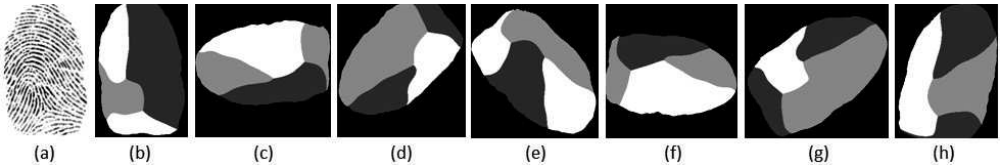


Figure 17: The different patterns produced when a 2 CR LL undergoes rotation at angles of (b)  $0^\circ$ , (c)  $90^\circ$ , (d)  $130^\circ$ , (e)  $220^\circ$ , (f)  $260^\circ$ , (g)  $300^\circ$  and (h)  $340^\circ$

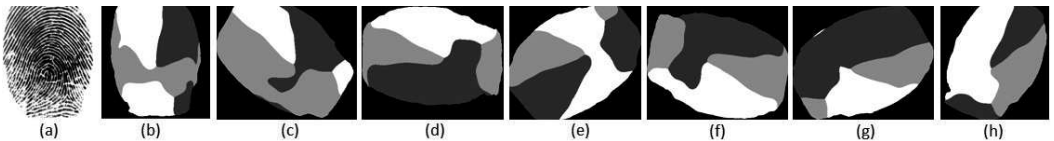


Figure 18: The DPs produced when a 1 CR LL undergoes rotation at angles of (b)  $10^\circ$ , (c)  $60^\circ$ , (d)  $90^\circ$ , (e)  $130^\circ$ , (f)  $260^\circ$ , (g)  $300^\circ$  and (h)  $340^\circ$

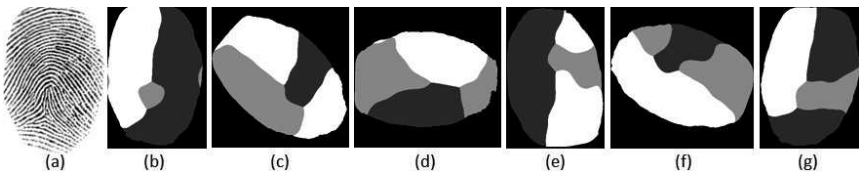


Figure 19: The different patterns produced when a 3 CR TA undergoes rotation at angles of (b)  $10^\circ$ , (c)  $50^\circ$ , (d)  $90^\circ$ , (e)  $190^\circ$ , (f)  $250^\circ$  and (g)  $350^\circ$

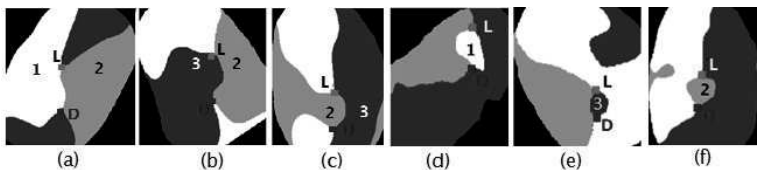


Figure 20: Fingerprint directional patterns produced when aligning SPs for a 2 CR layout (a) LL, (b) RL and (c) TA; and a 3 CR layout (d) LL, (e) RL and (f) TA

13 to 19 show a great variation of patterns under rotation. The number of CRs vary, for example a 2 CR pattern can change to a 3 CR pattern and as it varies the region numbers of the CRs change. Furthermore, RLs, LLs and TAs have highly similar patterns, since any of these classes with the same number of CRs, produce the same region number for the CRs, at each angle. This makes it difficult to differentiate between classes. Since it increases interclass variability among classes, classification accuracy is affected. The only visual difference between these classes, is the location of the SPs on the pattern. However, the location of SPs can only be used to differentiate the classes if fingerprints are all at the same rotation which is unlikely to occur. Therefore, in order to classify a RL, LL and TA consistently from the DPs, a particular method of rotation must be found that produces a unique pattern for each class. In addition, the method of rotation must not be reliant on the fingerprint being initially upright, as this is often not the case. Hence, the method of rotation cannot simply be a global angle to rotate by.

After, further analysing the DP under rotation, it was observed that when the SPs are aligned either vertically or horizontally, both of these requirements are achieved, i.e, a unique pattern is produced for each class and the rotation can be achieved consistently since it is based on internal landmarks rather than a global angle. This is shown by Figure 20, in which SPs are vertically aligned. Figure 20 (a) - Figure 20 (c) show a 2 CR pattern where a LL, RL and TA can be identified by unique region numbers: 1 and 2; 3 and 2; and 2 and 3, respectively. Figure 20 (d)- Figure 20 (f) shows a 3 CR pattern where a LL, RL and TA can be detected by the unique region number of the smallest CR being: 1; 2 and 3, respectively. Since it is independent of using the position of the SP to identify a class, it makes it more reliable by overcoming interclass variability issues and rotation. Therefore, a proposed solution to achieve consistency is to align the SPs.

## 4 Recommendation

Based on the findings in Section 3, the recommendation on the number of regions and amount of rotation for each class are as follows:-

1. A three region partition is recommended, since it produces distinct patterns with the highest SP detection accuracy compared to all other region quantities. Furthermore, the size of each region makes it easier to detect accurate SPs, to eliminate false SPs and noise.
2. For PAs and Ws, consistent patterns can be established at any rotation.
3. For RL, LL and TA fingerprints, vertically aligning the SPs is suggested. This produces consistent unique patterns consisting of only two types of layout, 2 CR and 3 CR.

## 5 Conclusion

This investigation focused on analysing the different DP layouts produced as the number of regions and rotation of the fingerprint was varied and which patterns represent the essential properties of a class better. It was found that a smaller number of regions produced higher accuracy of SP detection, since there are less regions at the point of intersection and they intersect at a single point. Furthermore, it was found that vertically aligning the SPs of a single loop and delta image produces consistent results with fewer possible layouts. The

region between the loop and delta is represented by a unique region number for a particular class type. Therefore, it does not rely only on the positioning of the SPs, making it less prone to interclass variability issues.

## References

- [BKAM13] G.A. Bahgat, A.H. Khalil, N.S. Abdel Kader, and S. Mashali. Fast and accurate algorithm for core point detection in fingerprint images. *Egypt. Informatics J.*, 14(1):15–25, March 2013.
- [CMM02] R. Cappelli, D. Maio, and D. Maltoni. Multi-Classifer Approach to Fingerprint Classification. *Pattern Anal. Appl.*, 5(2):136–144, 2002.
- [DWTk15] K. Dorasamy, L. Webb, J. Tapamo, and N. Khanyile. Fingerprint Classification using a Simplified Rule-Set based on Directional Patterns and Singularity Features. In *8th IAPR Int. Conf. Biometrics*, Phuket, Thailand, 2015. IEEE.
- [Gal91] F. Galton. The Patterns in Thumb and Finger Marks. On their Arrangement into naturally distinct Classes, the Permanence of the Papillary Ridges that make them, and the Resemblance of their Classes to Ordinary Genera. *Philos. Trans. R. Soc. London.B*, (January):1–25, 1891.
- [HWJ98] L. Hong, Y. Wan, and A. Jain. Fingerprint Image Enhancement : Algorithm and Performance Evaluation. 20(8):777–789, 1998.
- [LHH08] L. Liu, C. Huang, and D. C. D. Hung. Directional Approach to Fingerprint Classification. *Int. J. Pattern Recognit. Artif. Intell.*, 22(02):347–365, March 2008.
- [MM96] D. Maio and D. Maltoni. A Structural Approach to Fingerprint Classification. In *Proc. 13th Int. Conf. Pattern Recognit.*, pages 578–585, Italy, 1996. IEEE.
- [MMC<sup>+</sup>02] D. Maio, D. Maltoni, R. Cappelli, J. Wayman, and A. Jain. FVC2002: Second Fingerprint Verification Competition, 2002.
- [WBGs10] L. Wang, N. Bhattacharjee, G. Gupta, and B. Srinivasen. Adaptive approach to fingerprint image enhancement. In *Proc. 8th Int. Conf. Adv. Mob. Comput. Multimed.*, pages 42–49, 2010.
- [WBS12] L. Wang, N. Bhattacharjee, and B. Srinivasan. Fingerprint Reference Point Detection Based on Local Ridge Orientation Patterns of Fingerprints. In *WCCI 2012 IEEE World Congr. Comput. Intell.*, pages 10–15, Brisbans, Australia, 2012. IEEE.